

Sudden future singularities in quintessence and scalar-tensor quintessence models

A. Lympersis,^{1,*} L. Perivolaropoulos,^{1,2,†} and S. Lola^{1,‡}

¹*Department of Physics, University of Patras, 26500 Patras, Greece*

²*on leave from Department of Physics, University of Ioannina, Ioannina 45110, Greece*

(Received 10 July 2017; published 12 October 2017)

We demonstrate analytically and numerically the existence of geodesically complete singularities in quintessence and scalar-tensor quintessence models with scalar field potential of the form $V(\phi) \sim |\phi|^n$ with $0 < n < 1$. In the case of quintessence, the singularity which occurs at $\phi = 0$, involves divergence of the third time derivative of the scale factor [Generalized Sudden Future Singularity (GSFS)], and of the second derivative of the scalar field. In the case of scalar-tensor quintessence with the same potential and with a linear minimal coupling ($F(\phi) = 1 - \lambda\phi$), the singularity is stronger and involves divergence of the second derivative of the scale factor [Sudden Future Singularity (SFS)]. We show that the scale factor close to the singularity is of the form $a(t) = a_s + b(t_s - t) + c(t_s - t)^2 + d(t_s - t)^q$ where a_s, b, c, d are constants which are obtained from the dynamical equations and t_s is the time of the singularity. In the case of quintessence we find $q = n + 2$ (i.e. $2 < q < 3$), while for the case of scalar-tensor quintessence we have a stronger singularity with $q = n + 1$ ($1 < q < 2$). We verify these analytical results numerically and extend them to the case where a perfect fluid, with a constant equation of state $w = \frac{p}{\rho}$, is present. We find that the strength of the singularity (value of q) remains unaffected by the presence of a perfect fluid. The linear and quadratic terms in $(t_s - t)$ that appear in the expansion of the scale factor around t_s are subdominant for the diverging derivatives close to the singularity, but can play an important role in the estimation of the Hubble parameter. Using the analytically derived relations between these terms, we derive relations involving the Hubble parameter close to the singularity, which may be used as observational signatures of such singularities in this class of models. For quintessence with matter fluid, we find that close to the singularity $\dot{H} = \frac{3}{2}\Omega_{0m}(1 + z_s)^3 - 3H^2$. These terms should be taken into account when searching for future or past time such singularities, in cosmological data.

DOI: 10.1103/PhysRevD.96.084024

I. INTRODUCTION

The fact that the Universe has entered a phase of accelerating expansion ($\ddot{a} > 0$) [1,2] has created new possibilities in the context of the study of exotic physics on cosmological scales. Cosmological observations of Type Ia supernova [3], which were later supported by the cosmic microwave background (CMB) [4] and the large scale structure observations [5,6], are consistent with the existence of a cosmological constant (Λ CDM model) [7] as the possible cause of this mysterious phenomenon. Despite the simplicity of Λ CDM and its consistency with most cosmological observations [3] the required value of the cosmological constant needs to be fine-tuned in comparison with microphysical expectations. This problem has led to the consideration of models alternative to Λ CDM. Such models include modifications of GR [8,9], scalar field dark energy (quintessence) [10,11], physically motivated forms of fluids e.g. Chaplygin gas [12,13] etc.

Some of these dark energy models predict the existence of exotic cosmological singularities, involving divergences of the scalar spacetime curvature and/or its derivatives. These singularities can be either geodesically complete [14–17] (geodesics continue beyond the singularity and the Universe may remain in existence) or geodesically incomplete [18,19] (geodesics do not continue beyond the singularity and the Universe ends at the classical level). They appear in various physical theories such as superstrings [20], scalar field quintessence with negative potentials [21], modified gravities and others [17,22,23]. Violation of the cosmological principle (isotropy-homogeneity) by some cosmological models (e.g. modified gravity [24], quantum effects [25]), has been shown to eliminate or weaken both geodesically complete and incomplete singularities [26–45].

Geodesically incomplete singularities include the Big Bang [46], the Big Rip [47,48] where the scale factor diverges at a finite time due to infinite repulsive forces of phantom dark energy, the Little Rip [49] and the Pseudo Rip [50] singularities where the scale factor diverges at an infinite time and the Big Crunch [16,17,21,51–53] where the scale factor vanishes due to the strong attractive gravity

*alymperis@upatras.gr

†leandros@uoi.gr

‡magda@physics.upatras.gr

of future involved dark energy, as e.g. in quintessence models with negative potential.

Geodesically complete singularities include SFS (Sudden Future Singularity) [22], Big-Brake singularity [54] (a subclass of the SFS singularities, characterized by a full stop of the expansion with finite scale factor, vanishing energy density and diverging deceleration and pressure), FSF (Finite Scale Factor) [55,56], BS (Big-Separation) and the w-singularity [57,58]. In these singularities, the cosmic scale factor remains finite but a scale factor's derivative diverges at a finite time. The singular nature of these "singularities" amounts to the divergence of scalar quantities involving the Riemann tensor and the Ricci scalar $R = 6(\frac{\ddot{a}}{a} + \frac{\dot{a}^2}{a^2} + \frac{k}{a^2})$, for the FRW metric, where $a(t)$ is the cosmic scale factor [59]. Despite the divergence of the Ricci scalar, the geodesics are well defined at the time of the singularity. The Tipler and Krolak [60,61] integrals of the Riemann tensor components along the geodesics are indicators of the strength of these singularities and remain finite in most cases. The Tipler integral [60] is defined as

$$\int_0^\tau d\tau' \int_0^{\tau'} d\tau'' |R_{0j0}^i(\tau'')|, \quad (1.1)$$

while the Krolak integral [61] is defined as

$$\int_0^\tau d\tau' |R_{0j0}^i(\tau')|, \quad (1.2)$$

where τ is the affine parameter along the geodesic and R_{0j0}^i is the Riemann tensor. The components of the Riemann tensor are expressed in a frame that is parallel transported along the geodesics. If the scale factor's first derivative is finite at the singularity, both integrals are finite (even if the second derivative of the scale factor diverges), since the Riemann tensor components involve up to second order derivatives of the scale factor. If, however, the first derivative of the finite scale factor diverges, then it is easy to see from the above integrals that only the Tipler integral is finite at the singularity, while the Krolak integral diverges. This implies an infinite impulse on the geodesics, which dissociate all bound systems at the time of the singularity [15,62]. The singularities that lead to the divergence of the above integrals are defined as *strong singularities* [63,64].

It is interesting to connect these singularities with the properties of the cosmic energy-momentum tensor. In FRW spacetime with metric

$$ds^2 = -dt^2 + a^2(t) \left[\frac{dr^2}{1 - kr^2} + r^2(d\theta^2 + \sin^2\theta d\phi^2) \right], \quad (1.3)$$

and we assume the standard Einstein-Hilbert action

$$S = \int \left[\frac{1}{16\pi G} R + \mathcal{L}_{(\text{fluid})} \right] \sqrt{-g} d^4x. \quad (1.4)$$

The Friedmann equations obtained by variation of the above action connect the density and pressure with the cosmic scale factor $a(t)$:

$$\rho(t) = \frac{3}{8\pi G} \left(\frac{\dot{a}^2}{a^2} + \frac{k}{a^2} \right) \quad (1.5)$$

$$p(t) = -\frac{1}{8\pi G} \left(2\frac{\ddot{a}}{a} + \frac{\dot{a}^2}{a^2} + \frac{k}{a^2} \right), \quad (1.6)$$

where the density and pressure are connected by the continuity equation:

$$\dot{\rho}(t) = -3\frac{\dot{a}}{a}[\rho(t) + p(t)]. \quad (1.7)$$

In what follows we set $8\pi G = c = 1$ and assume spatial flatness ($k = 0$), in agreement with observational results and the WMAP [65].

The divergence of the scale factor and/or its derivatives leads to divergence of scalar quantities like the Ricci scalar thus to different types of singularities or "cosmological milestones" [59]. However geodesics do not necessarily end at these singularities and if the scale factor remains finite they are extended beyond these events [23] even though a diverging impulse may lead to dissociation of all bound systems in the Universe at the time t_s of these events [62].

Thus singularities can be classified [66] according to the behavior of the scale factor $a(t)$, and/or its derivatives at the time t_s of the event or equivalently [according to Eqs. (1.5)–(1.6)] and the energy density and pressure of the content of the universe at the time t_s . A classification of such singularities and their properties is shown in Table I.

A particularly interesting type of singularity is the Sudden Future Singularity [22], which involves violation of the dominant energy condition $\rho \geq |p|$, and divergence of the cosmic pressure of the Ricci Scalar and of the second time derivative of the cosmic scale factor. The scale factor can be parametrized as

$$a(t) = \left(\frac{t}{t_s} \right)^m (a_s - 1) + 1 - \left(1 - \frac{t}{t_s} \right)^q, \quad (1.8)$$

where m, q, t_s are constants to be determined, a_s is the scale factor at the time t_s and $1 < q < 2$. The idea of such a finite time singularity and the above asymptotic form of $a(t)$ was first introduced in [67], where it was used to show that closed FRW universes satisfying the strong energy condition $\rho + 3p \geq 0$, do not always recollapse. An interesting feature of such singularities includes the possibility for a quasi-isotropic solution which is part of the general solution of the Einstein equations, and approaches a late-time sudden singularity where the density, expansion rate, and metric

TABLE I. Classification and properties of cosmological singularities. The singularities discussed in the present analysis are indicated in italics.

Name	t_{sing}	$a(t_s)$	$\rho(t_s)$	$p(t_s)$	$\dot{p}(t_s)$	$w(t_s)$	T	K	Geodesically
Big Bang (BB)	0	0	∞	∞	∞	finite	strong	strong	incomplete
Big Rip (BR)	t_s	∞	∞	∞	∞	finite	strong	strong	incomplete
Big Crunch (BC)	t_s	0	∞	∞	∞	finite	strong	strong	incomplete
Little Rip (LR)	∞	∞	∞	∞	∞	finite	strong	strong	incomplete
Pseudo Rip (PR)	∞	∞	finite	finite	finite	finite	weak	weak	incomplete
<i>Sudden future (SFS)</i>	t_s	a_s	ρ_s	∞	∞	finite	weak	weak	complete
Big Brake (BBS)	t_s	a_s	0	∞	∞	finite	weak	weak	complete
Finite sudden future (FSF)	t_s	a_s	∞	∞	∞	finite	weak	strong	complete
<i>Generalized sudden future (GSFS)</i>	t_s	a_s	p_s	p_s	∞	finite	weak	strong	complete
Big separation (BS)	t_s	a_s	0	0	∞	∞	weak	weak	complete
w-singularity (w)	t_s	a_s	0	0	0	∞	weak	weak	complete

remain finite. This solution has no equation of state and is characterized by nine independent arbitrary spatial functions [68]. In addition to (1.8) there are other similar parametrizations of the scale factor for sudden future singularities, which are also applicable for Big Bang, Big Rip, sudden future, finite scale factor and w -singularities [69,70].

For the range $1 < q < 2$, Eq. (1.8) indicates that a, \dot{a} and ρ remain finite at t_s . However, from Eqs. (1.6)–(1.7) it follows that p, \dot{p} and \ddot{a} become infinite. Thus, when the first derivative of the scale factor is finite at the singularity, but the second derivative diverges (SFS singularity [22]), the energy density is finite but the pressure diverges. SFS singularities ($p \rightarrow +\infty, \ddot{a} \rightarrow -\infty$) violate only the dominant energy condition (DEC: $\rho \geq |p|$) while it respects all other energy conditions [null energy condition (NEC): $\rho + p \geq 0$], weak energy condition (WEC): $\rho \geq 0, \rho + p \geq 0$, strong energy condition (SEC): $\rho + 3p \geq 0$].

Geodesically complete singularities where the scale factor behaves like Eq. (1.8), are obtained in various physical models such as, anti-Chaplygin gas [71,72], loop quantum gravity [45], tachyonic models [35–37,54], brane models [32,73,74] etc. Such singularities however have not been studied in detail in the context of the simplest dark energy models of quintessence and scalar-tensor quintessence (see however [75,76] for a qualitative analysis in the case of inflation).

A singularity of the GSFS type (see Table I), involving a divergence of the third derivative of the scale factor, occurs generically in quintessence models with potential of the form

$$V(\phi) = A|\phi|^n, \quad A > 0, \quad (1.9)$$

with $0 < n < 1$ and A a constant parameter. In Ref. [75], it was shown through a qualitative analysis, that the power law scalar potential leads to singularities at any scale factor derivative order larger than three, depending on the value of the power n . In particular, for $k < n < k + 1$, with $k > 0$, the $(k + 2)^{\text{th}}$ derivative of the scale factor diverges at the singularity. Quintessence models with the potential (1.9)

constitute the simplest extension of Λ CDM with geodesically complete cosmic singularities that occur at the time t_s when the scalar field becomes zero ($\phi = 0$).

In the present study we extend the analysis of [75,76] in the following directions:

- (1) We verify the existence of the GSFS both numerically and analytically, using a proper generalized expansion ansatz for the scale factor and the scalar field close to the singularity. This generalized ansatz includes linear and quadratic terms, that dominate close to the singularity and cannot be ignored when estimating the Hubble parameter and the scalar field energy density. Thus, they are important when deriving the observational signatures of such singularities.
- (2) We derive analytical expressions for the power (strength) of the singularity in terms of the power n of the scalar field potential.
- (3) We extend the analysis to the case of scalar-tensor quintessence with the same scalar field potential and derive both analytically and numerically the power of the singularity in terms of the power n of the scalar field potential.

The structure of this paper is the following: In Sec. II we focus on the quintessence model of Eq. (1.9), and we investigate the strength of the GSFS both analytically and numerically. In Sec. III we extend the analysis to the case of scalar-tensor quintessence and investigate the modification of the strength of the singularity both analytically (using a proper expansion ansatz) and numerically, by explicitly solving the dynamical cosmological equations. Finally, in Sec. IV we summarize our results and discuss possible extensions of the present analysis.

II. SUDDEN FUTURE SINGULARITIES IN QUINTESSENCE MODELS

A. Evolution without perfect fluid

Setting $8\pi G = 1$, the most general action, involving gravity, nonminimally coupled with a scalar field ϕ , and a perfect fluid is

$$\mathcal{S} = \int \left[\frac{1}{2} F(\phi) R + \frac{1}{2} g^{\mu\nu} \phi_{;\mu} \phi_{;\nu} - V(\phi) + \mathcal{L}_{(\text{fluid})} \right] \sqrt{-g} d^4x. \quad (2.1)$$

In the special case where $F(\phi) = 1$ and in the absence of a perfect fluid, the action (2.1) reduces to the simple case of quintessence models without a perfect fluid

$$\mathcal{S} = \int \left[\frac{1}{2} R + \frac{1}{2} g^{\mu\nu} \phi_{;\mu} \phi_{;\nu} - V(\phi) \right] \sqrt{-g} d^4x. \quad (2.2)$$

The energy density and pressure of the scalar field ϕ , may be written as

$$\rho_\phi = \frac{1}{2} \dot{\phi}^2 + V(\phi) \quad \text{and} \quad p_\phi = \frac{1}{2} \dot{\phi}^2 - V(\phi). \quad (2.3)$$

Variation of the action (2.2) assuming a power law potential (1.9) leads to the dynamical equations

$$3H^2 = \frac{1}{2} \dot{\phi}^2 + V(\phi) \quad (2.4)$$

$$\ddot{\phi} = -3H\dot{\phi} - An|\phi|^{n-1}\Theta(\phi) \quad (2.5)$$

$$2\dot{H} = -\dot{\phi}^2, \quad (2.6)$$

where $H = \frac{\dot{a}}{a}$ is the Hubble parameter, $0 < n < 1$ and

$$\Theta(\phi) = \begin{cases} 1 & \phi > 0 \\ -1 & \phi < 0 \end{cases}. \quad (2.7)$$

This class of quintessence models has been studied extensively focusing mostly on the cosmological effects and the dark energy properties that emerge due to the expected oscillations of the scalar field around the minimum of its potential [77–81]. In the present analysis we focus instead on the properties of the cosmological singularity that is induced as the scalar field vanishes periodically during its oscillations. For simplicity, we consider only the first time t_s when the scalar field vanishes during its dynamical oscillations. Notice that the discontinuity of Eq. (2.5) is mild for $0 < n < 1$ and is integrated out in the solution leading to no issues with instabilities or divergences.

The dynamical evolution of the scalar field due to the potential shown in Fig. 1 may be qualitatively described as follows [76]:

From Eqs. (2.4) and (2.6), it follows that when $t \rightarrow t_s$ ($\phi \rightarrow 0$) H, \dot{H} remain finite and so does $\dot{\phi}$. But in Eq. (2.5) there is a divergence of the term ϕ^{n-1} for $0 < n < 1$ and thus $\ddot{\phi} \rightarrow \infty$ as $\phi \rightarrow 0$. \ddot{H} also diverges at this point due to the divergence of $\ddot{\phi}$, as follows by differentiating Eq. (2.6). This implies that the third derivative of the scale factor

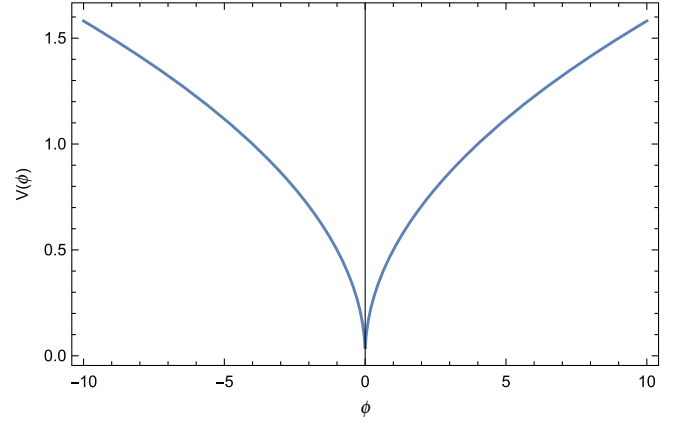


FIG. 1. Exponential scalar field potential $V(\phi) = A|\phi|^n$.

diverges, and a GSFS occurs at this point (i.e. a_s, ρ_s, p_s remain finite but $\dot{p} \rightarrow \infty$). Thus, the constraints on the power exponents q, r of the diverging terms in the expansion of the scale factor ($\sim (t_s - t)^q$) and of the scalar field ($\sim (t_s - t)^r$) are $2 < q < 3$ and $1 < r < 2$ respectively [see Eqs. (2.10)–(2.11) below]. It has been shown in [82] that by choosing q to lie in the intervals $(N, N + 1)$ for $N \geq 2$, where $N \in \mathbb{Z}^+$, a finite-time singularity occurs in which

$$\frac{d^{N+1}a}{dt^{N+1}} \rightarrow \infty, \quad (2.8)$$

while

$$\frac{d^s a}{dt^s} \rightarrow 0, \quad \text{for } s \leq N \in \mathbb{Z}^+. \quad (2.9)$$

It may be shown that this allows for pressure singularities which are associated with divergence of higher time derivatives of the scale factor (divergence of the fourth-order derivative of the scale factor [82] when $p \rightarrow \infty$), in Friedmann solutions of higher-order gravity [$f(R)$] theories [83].

In what follows we extend the above qualitative analysis to a quantitative level. In particular, we use a new ansatz for the scale factor and the scalar field, containing linear and quadratic terms of $(t_s - t)$. These terms play an important role since they dominate in the first and second derivative of the scale factor as the singularity is approached.

Thus, the new ansatz for the scale factor which generalizes (1.8), by introducing linear and quadratic terms in $(t_s - t)$ is of the form

$$a(t) = a_s + b(t_s - t) + c(t_s - t)^2 + d(t_s - t)^q, \quad (2.10)$$

where b, c, d are real constants to be determined, and $2 < q < 3$ so that \ddot{a} diverges at the GSFS. In [68], it has been shown that an asymptotic series for a general solution

of the Einstein equations, can be constructed near a sudden singularity. In our parametrization (2.10), we keep only the terms that can play an important role close to the singularity.

The corresponding expansion of the scalar field $\phi(t)$ close to singularity is of the form

$$\phi(t) = f(t_s - t) + h(t_s - t)^r, \quad (2.11)$$

where f , h , are real constants to be determined, and $1 < r < 2$ so that $\ddot{\phi}$ diverges at the singularity.

Substituting Eqs. (2.10) and (2.11) in Eq. (2.5), we get the equation of the dominant terms

$$\mathcal{A}_1(t_s - t)^{r-2} = \mathcal{A}_2(t_s - t)^{n-1}, \quad (2.12)$$

where the \mathcal{A}_1 , \mathcal{A}_2 , denote constants, which may be expressed in terms of f , h and the constant A (see Appendix). Clearly, both the left and right-hand side of Eq. (2.12) diverge at the singularity for $1 < r < 2$ and $0 < n < 1$. Equating the power laws of divergent terms we obtain

$$r = n + 1. \quad (2.13)$$

Similarly, differentiation of Eq. (2.6) with respect to t gives $2\dot{H} = -2\dot{\phi}\ddot{\phi}$, from which we obtain an equation for the dominant terms using Eqs. (2.10) and (2.11)

$$\mathcal{A}'_1(t_s - t)^{q-3} = \mathcal{A}'_2(t_s - t)^{r-2}, \quad (2.14)$$

where the \mathcal{A}'_1 , \mathcal{A}'_2 are constants, which may be expressed in terms of d , f , h (see Appendix). The left and the right-hand side of Eq. (2.14) diverge, and therefore, equating the power laws of diverging terms we obtain

$$q = r + 1. \quad (2.15)$$

Thus, using (2.13) and (2.15) we find the exponent q in terms of n as

$$q = n + 2. \quad (2.16)$$

Equations (2.13) and (2.16) are consistent with the qualitatively expected range of r , q , for $0 < n < 1$.

Substituting the expressions (2.10), (2.11), (1.9) for $a(t)$, $\phi(t)$ and $V(\phi)$ in the dynamical Eqs. (2.4) and (2.6), it is straightforward to calculate the relations between the coefficients c , d , f , h . The form of the relations between the evaluated expansion coefficients, is shown in the Appendix, and has been verified by numerical solution of the dynamical equations.

The additional linear and quadratic terms in $(t_s - t)$, in the expression of the scale factor (2.10), play an important role in the estimation of the Hubble parameter and its derivative as the singularity is approached.

The relations between these coefficients can lead to relations between the Hubble parameter and its derivative

close to the singularity, which in turn correspond to observational predictions that may be used to identify the presence of these singularities in angular diameter of luminosity distance data. For example, the coefficients b and c are related as [see Appendix Eq. (A2)],

$$c = -\frac{b^2}{a_s}. \quad (2.17)$$

Using this relation, it is easy to show that at the time of the singularity t_s we have

$$\dot{H} = -3H^2. \quad (2.18)$$

Equation (2.18) is identical to the corresponding equation describing a stiff matter fluid with $\rho = p$.

The solution of Eq. (2.18) expressed in terms of redshift z , is applicable at the singularity redshift z_s and may be written as

$$H(z_s) = (1 + z_s)^3. \quad (2.19)$$

This result constitutes an observationally testable prediction of this class of models, which can be used to search for such singularities in our past light cone.

B. Numerical analysis

It is straightforward to verify numerically the derived power law dependence of the scale factor and scalar field as the singularity is approached. We thus solve the rescaled, with the present day Hubble parameter H_0 (setting $H = \bar{H}H_0$, $t = \bar{t}/H_0$, $V = \bar{V}H_0^2$), coupled system of the cosmological dynamical equations for the scale factor and for the scalar field (2.5) and (2.6). We assume initial conditions at early times ($t \ll t_0$) when the scalar field is assumed frozen at $\phi(t_i) = \phi_i$ and $\dot{\phi}(t_i) = 0$ due to cosmic friction [84,85]. At that time the initial conditions for the scale factor are well approximated by

$$a(t_i) = \exp \left[\sqrt{\frac{V(\phi_i)}{3}} t_i \right], \quad (2.20)$$

$$\dot{a}(t_i) = \sqrt{\frac{V(\phi_i)}{3}} \left[\exp \sqrt{\frac{V(\phi_i)}{3}} t_i \right]. \quad (2.21)$$

Taking the logarithm of the numerical solution corresponding to the third derivative of the scale factor (2.10) and to the second derivative of the scalar field (2.11), we obtain Fig. 2 and Fig. 3, which show these logarithms as functions of $t_s - t$ close to the singularity (continuous lines). On these lines we superpose the corresponding analytic expansions [Eqs. (2.10) and (2.11), dashed lines] which, close to the singularity, may be written as

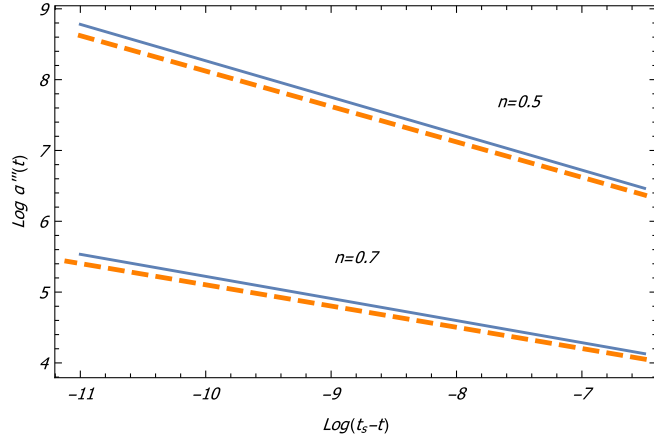


FIG. 2. Numerical verification of the q -exponent for $n = 0.5$ and $n = 0.7$. The orange dashed line, denotes the analytical, while the blue line denotes the numerical solution. As expected the slopes for each n are identical.

$$\log[|\ddot{a}|] = \log[d|q(q-1)(q-2)|] + (q-3)\log[(t_s-t)] \quad (2.22)$$

and

$$\log[|\dot{\phi}|] = \log[h|r(r-1)|] + (r-2)\log[(t_s-t)]. \quad (2.23)$$

In the plots of Eqs. (2.22)–(2.23) (dashed lines) we have used the predicted values of the exponents [Eqs. (2.13) and (2.16)] and the analytically predicted values for the coefficients d and h shown in the Appendix. We underline the good agreement in the slopes of the analytically predicted curves and the corresponding numerical results, which confirm the validity of the power law ansatz (2.10) and (2.11), and the values of the corresponding exponents (2.13) and (2.16).

We have also verified this agreement by obtaining the best fit slopes of the numerical solutions of Fig. 2 and Fig. 3

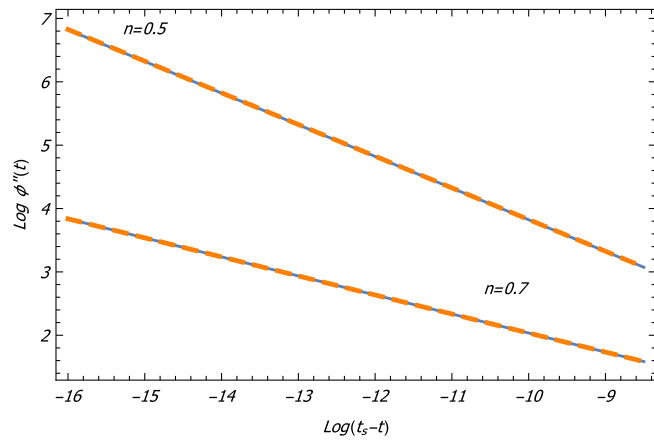


FIG. 3. Same as Fig. 2 for the r -exponent.

TABLE II. Numerical and analytical values of the power exponents r , q . Clearly, there is consistency between numerical results and analytical expectations.

n	Numerical		Analytical	
	r	q	$r = n + 1$	$q = n + 2$
0.5	1.5 ± 0.0003	2.51 ± 0.0007	1.5	2.5
0.7	1.7 ± 0.002	2.71 ± 0.004	1.7	2.7

deriving the numerically predicted values of the exponents q and r . These numerical best fit values, along with the corresponding analytical predictions, are shown in Table II for $n = 0.5$ and $n = 0.7$, indicating good agreement between the analytical and numerical values of the exponents.

In Fig. 4 and Fig. 5 we show the time evolution (numerical and analytical) of the scale factor and the scalar field respectively. The two curves, for each n , are consistent close to each singularity. In Fig. 6 and Fig. 7 we demonstrate numerically the divergence of the third derivative of the scale factor and of the second derivative of the scalar field. The divergence occurs at the time of the singularity when the scalar field vanishes i.e. $\phi = 0$.

C. Evolution with a perfect fluid

In the presence of a perfect fluid, the action of the theory is obtained from the generalized action (2.1) with $F(\phi) = 1$ as

$$\mathcal{S} = \int \left[\frac{1}{2}R + \frac{1}{2}g^{\mu\nu}\phi_{;\mu}\phi_{;\nu} - V(\phi) + \mathcal{L}_{(\text{fluid})} \right] \sqrt{-g}d^4x. \quad (2.24)$$

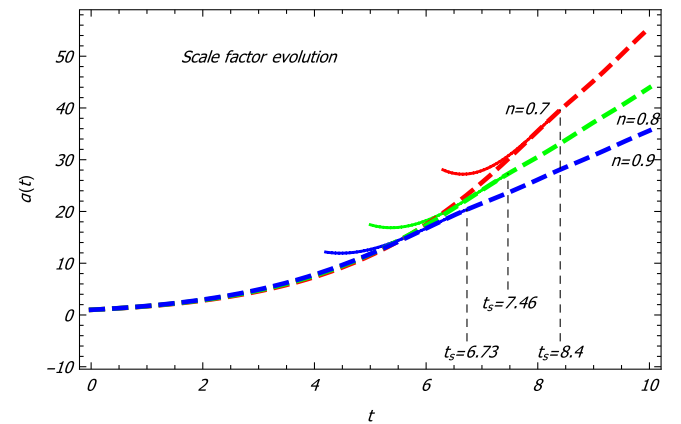


FIG. 4. Plot of numerical (dashed) and analytical (line) time evolution of the scale factor, for $n = 0.7, 0.8, 0.9$. The two solutions for each n are consistent close to each singularity.

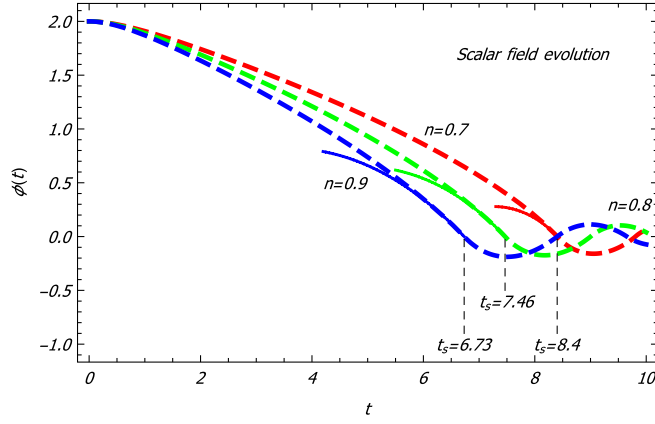


FIG. 5. Numerical (dashed line) and analytical (continuous line) time evolution of the scalar field, for $n = 0.7, 0.8, 0.9$. The two solutions for each n are consistent close to each singularity.

The corresponding dynamical equations are

$$3H^2 = \frac{3\Omega_{0,m}}{a^3} + \frac{1}{2}\dot{\phi}^2 + V(\phi) \quad (2.25)$$

$$\ddot{\phi} = -3H\dot{\phi} - An|\phi|^{n-1}\Theta(\phi) \quad (2.26)$$

$$2\dot{H} = -\frac{3\Omega_{0,m}}{a^3} - \dot{\phi}^2, \quad (2.27)$$

with $\rho_m = \frac{\rho_{0m}}{a^3} = \frac{3\Omega_{0,m}}{a^3}$ and $\Omega_{0,m} = 0.3$. The scale factor (2.10), in the presence of a perfect fluid is now assumed to be of the form

$$a(t) = 1 + (a_s - 1)\left(\frac{t}{t_s}\right)^m + b(t_s - t) + c(t_s - t)^2 + d(t_s - t)^q, \quad (2.28)$$

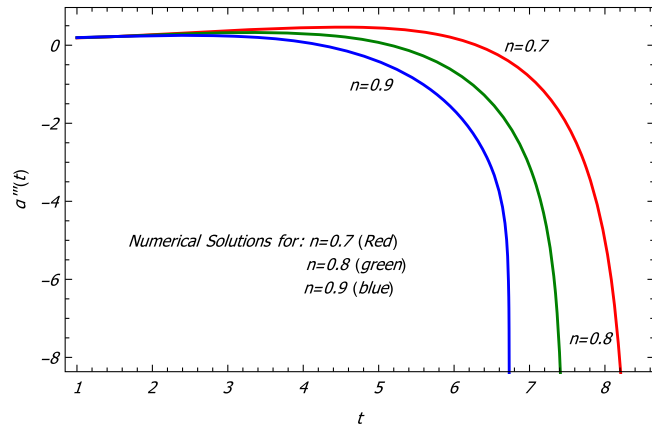


FIG. 6. Numerical solutions of the third time derivative of the scale factor for $n = 0.7, 0.8, 0.9$. Notice the divergence at the time of the singularity when the scalar field vanishes ($t_s = 8.4$ for $n = 0.7$, $t_s = 7.46$ for $n = 0.8$, $t_s = 6.73$ for $n = 0.9$).

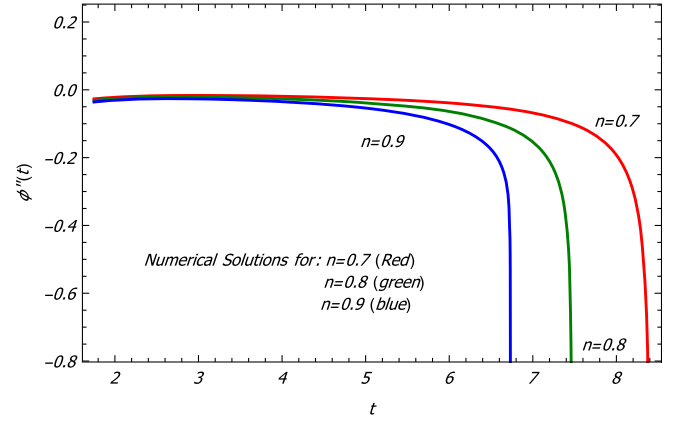


FIG. 7. Numerical solutions of the second time derivative of the scalar field for $n = 0.7, 0.8, 0.9$. Notice the divergence at the time of the singularity when the scalar field vanishes ($t_s = 8.4$ for $n = 0.7$, $t_s = 7.46$ for $n = 0.8$, $t_s = 6.73$ for $n = 0.9$).

where $m = \frac{2}{3(1+w)}$ and w the state parameter. As in the case of the previous section, from the dynamical equations (2.25), (2.27), $H, \dot{H}, \dot{\phi}$ still remain finite. Also in Eq. (2.26) there is a divergence of the term ϕ^{n-1} for $0 < n < 1$ and $\ddot{\phi} \rightarrow \infty$ as $\phi \rightarrow 0$. The third derivative of the scale factor \ddot{a} also diverges due to the divergence of \ddot{H} (differentiation of Eq. (2.6)). Thus, the constraints for q, r are the same as in the absence of the fluid (Sec. II A), i.e. $2 < q < 3$ and $1 < r < 2$ respectively.

Following the steps of Sec. II A, we rediscover the same values for the exponents i.e. Eqs. (2.13) and (2.16) which imply similar behavior close to the singularity.

The relations among the expansion coefficients c, d, f, h , are shown in the Appendix, and have been verified by numerical solution of the dynamical equations, as in the absence of the fluid (see Appendix). For $\rho_{0m} = 0$ all coefficients reduce to those of the no fluid case.

An interesting result arises from the derivation of the relation between the coefficients b, c . The relation between b, c in the presence of a fluid is of the form [see Appendix Eq. (A10)],

$$c = \frac{\rho_{0,m}}{4a_s^2} - \frac{1}{2}(a_s - 1)m(m - 1) - \frac{[(a_s - 1)m - b]^2}{a_s}, \quad (2.29)$$

Thus, we obtain

$$\dot{H} = \frac{3\Omega_{0,m}}{2a_s^3} - 3H^2. \quad (2.30)$$

Solving Eq. (2.30), we obtain the Hubble parameter H as a function of the singularity redshift z_s as

$$H^2(z_s) = \Omega_{0,m}(1+z_s)^3[1 - (1+z_s)^3] + (1+z_s)^6, \quad (2.31)$$

(see proof in Appendix). Clearly Eq. (2.30) reduces to Eq. (2.19) for $\rho_{0,m} = 0$. This result may be used as observational signature of such singularities in this class of models.

III. SUDDEN FUTURE SINGULARITIES IN SCALAR-TENSOR QUINTESSENCE MODELS

A. Evolution without a perfect fluid

We now consider now scalar-tensor quintessence models without the presence of a perfect fluid. The action of the theory is the generalized action (2.1), where $\mathcal{L}_{(\text{fluid})}$ is ignored. Therefore, it has the form

$$S = \int \left[\frac{1}{2} F(\phi) R + \frac{1}{2} g^{\mu\nu} \phi_{;\mu} \phi_{;\nu} - V(\phi) \right] \sqrt{-g} d^4x. \quad (3.1)$$

We assume a nonminimal coupling linear in the scalar field $F(\phi) = 1 - \lambda\phi$ even though our results about the type of the singularity in this class of models is unaffected by the particular choice of the nonminimal coupling. The dynamical equations are of the form

$$3FH^2 = \frac{\dot{\phi}^2}{2} + V - 3H\dot{F} \quad (3.2)$$

$$\ddot{\phi} + 3H\dot{\phi} - 3F_\phi \left(\frac{\ddot{a}}{a} + H^2 \right) + An|\phi|^{(n-1)}\Theta(\phi) = 0 \quad (3.3)$$

$$-2F \left(\frac{\ddot{a}}{a} - H^2 \right) = \dot{\phi}^2 + \ddot{F} - H\dot{F}, \quad (3.4)$$

where $F_\phi = \frac{d}{d\phi} F$. From Eq. (3.2), it is clear that $H, \dot{\phi}, F, \dot{F}$ all remain finite when $\phi \rightarrow 0$ ($t \rightarrow t_s$). However, in Eq. (3.3) there is a divergence of the term V_ϕ for $0 < n < 1$ and $\ddot{\phi} \rightarrow \infty$ as $\phi \rightarrow 0$. This means that $\ddot{F} \rightarrow \infty$ because of the generation of the second derivative of ϕ that leads to a divergence of \ddot{a} in Eq. (3.4). The effective dark energy density and pressure take the form [17,86]

$$\rho_{\text{DE}} = \frac{\dot{\phi}^2}{2} + V - 3FH^2 - 3H\dot{F} \quad (3.5)$$

$$p_{\text{DE}} = \frac{\dot{\phi}^2}{2} - V - (2\dot{H} - 3H^2)F + \ddot{F} + 2H\dot{F}. \quad (3.6)$$

Thus ρ_{DE} remains finite in Eq. (3.5), while $p_{\text{DE}} \rightarrow \pm\infty$ in Eq. (3.6). Clearly, an SFS singularity (Table I, see also [87]) is expected to occur in scalar-tensor quintessence models, as opposed to the GSFS singularity in the corresponding

quintessence models. This result will be verified quantitatively in what follows.

Using the ansatz (2.10) and (2.11) in the dynamical Eq. (3.4) we find that the dominant terms close to the singularity are

$$\mathcal{B}_1(t_s - t)^{q-2} = \mathcal{B}_2(t_s - t)^{r-2}, \quad (3.7)$$

where the $\mathcal{B}_1, \mathcal{B}_2$ are constants, which depend on the coefficient d, h and the λ constant, and are shown in the Appendix. It immediately follows from Eq. (3.7) that

$$q = r. \quad (3.8)$$

Similarly, substituting the ansatz (2.10) and (2.11) in Eq. (3.3) we find that the dominant terms close to the singularity obey the equation

$$\mathcal{B}'_1(t_s - t)^{r-2} = \mathcal{B}'_2(t_s - t)^{n-1}, \quad (3.9)$$

where the $\mathcal{B}'_1, \mathcal{B}'_2$ are constants, which depend on the coefficient f and the constants A, λ as shown in the Appendix. Equating the exponents of the divergent terms we find

$$r = n + 1, \quad (3.10)$$

which leads to

$$q = n + 1. \quad (3.11)$$

The results (3.10) and (3.11) are consistent with the above qualitative discussion for the expected strength of the singularity. Thus in the case of the scalar-tensor theory we have a stronger singularity at t_s , compared to the singularity that occurs in quintessence models. This is a general result, valid not only for the coupling constant of the form $F = 1 - \lambda\phi$ but also for other forms of $F(\phi)$ (e.g. $F \sim \phi^r$), because the second derivative of F with respect to time, in the dynamical equations, will always generate a second derivative of ϕ with divergence, leading to a divergence of \ddot{a} .

Using Eqs. (3.2), (3.7), (3.8), (3.9), and (3.10), we calculate relations among the coefficients c, d, f, h . The form of these relations, is shown in the Appendix, and has been verified by numerical solution of the dynamical equations. Notice that all coefficients, except d , reduce to those of Sec. II A for $\lambda = 0$.¹

¹The coefficient d differs in scalar-quintessence since the divergence occurs in the second, instead of the third derivative of the scale factor.

B. Numerical analysis

We now solve the rescaled coupled system of the cosmological dynamical equations for the scale factor and for the scalar field (3.3) and (3.4), using the present day Hubble parameter H_0 (setting $H = \bar{H}H_0$, $t = \bar{t}/H_0$, $V = \bar{V}H_0^2$). We assume initial conditions at early times ($t \ll t_0$) when the scalar field is assumed frozen at $\phi(t_i) = \phi_i$ and $\dot{\phi}(t_i) = 0$ due to cosmic friction in the context of thawing [84,85] scalar-tensor quintessence [88–90]. At that time the initial conditions for the scale factor are

$$a(t_i) = \exp \left[\sqrt{\frac{V(\phi_i)}{3F_i}} t_i \right], \quad (3.12)$$

$$\dot{a}(t_i) = \exp \left[\sqrt{\frac{V(\phi_i)}{3F_i}} t_i \right] \sqrt{\frac{V(\phi_i)}{3F_i}}, \quad (3.13)$$

where $F_i = 1 - \lambda\phi_i$.

Taking the logarithm of the second derivative of the scale factor (2.10) and of the scalar field (2.11), we obtain

$$\log[|\ddot{a}|] = \log[|d|q(q-1)] + (q-2) \log[(t_s - t)] \quad (3.14)$$

and

$$\log[|\ddot{\phi}|] = \log[|h|r(r-1)] + (r-2) \log[(t_s - t)] \quad (3.15)$$

The numerical verification of the validity of Eqs. (3.10)–(3.11) has been performed similarly to the case of minimally coupled quintessence. In Fig. 8 and Fig. 9 we show the analytical and numerical solutions, for the logarithm of the diverging terms of the scale factor and the scalar field respectively, as $t \rightarrow t_s$ from below. The log-plots of the

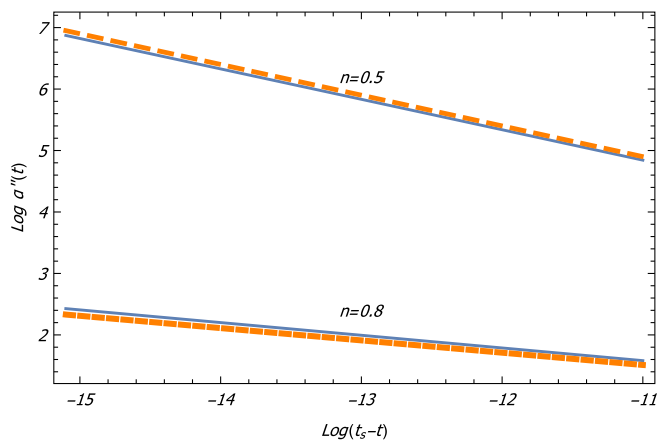


FIG. 8. Numerical verification of the q -exponent for $n = 0.5$ and $n = 0.8$. The orange dashed line, denotes the analytical, while the blue line denotes the numerical solution. As expected the slopes for each n are identical, while the small difference is due to the coefficients.

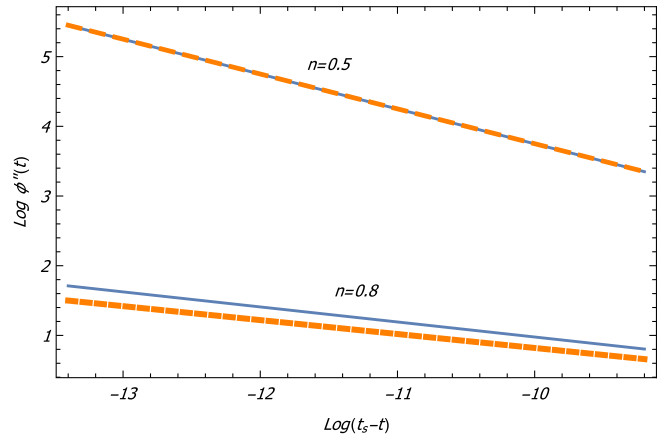


FIG. 9. Numerical verification of the r -exponent for $n = 0.5$ and $n = 0.8$. The orange dashed line, denotes the analytical, while the blue line denotes the numerical solution. As expected the slopes for each n are identical, while the small difference is due to the coefficients.

diverging terms of \ddot{a} and $\ddot{\phi}$ are straight lines, indicating a power law behavior with best fit slopes as shown in Table III, in good agreement with the analytical expansion expectations [Eqs. (3.10)–(3.11)]. In Figs. 10 and 11 we show the time evolution (numerical and analytical) of the scale factor and the scalar field respectively. The two curves, for each n , are consistent close to each singularity. In Figs. 12 and 13 we demonstrate numerically the divergence of the second derivative of the scale factor and of the scalar field. As expected, the divergence occurs at the time of the singularity when the scalar field vanishes.

Using Eqs. (3.14) and (3.15), it is straightforward to obtain numerically the values of the parameters h of the scalar field, as well as d of the scale factor, and compare with their analytically obtained values shown in the Appendix.

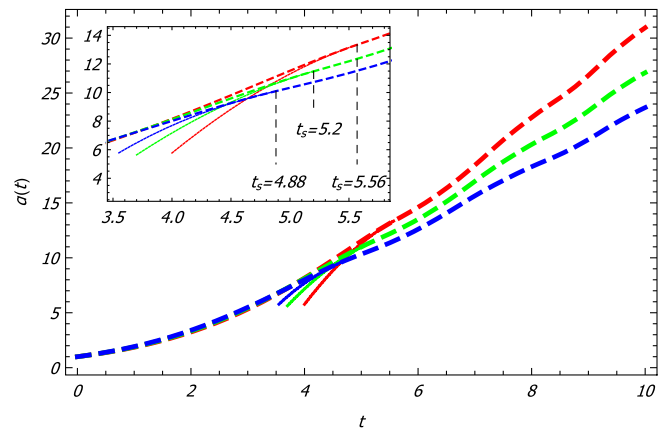


FIG. 10. Plot of numerical (dashed) and analytical (line) time evolution of the scale factor, for $n = 0.7$ (red), 0.8 (green), and 0.9 (blue). The two solutions for each n are consistent close to each singularity.

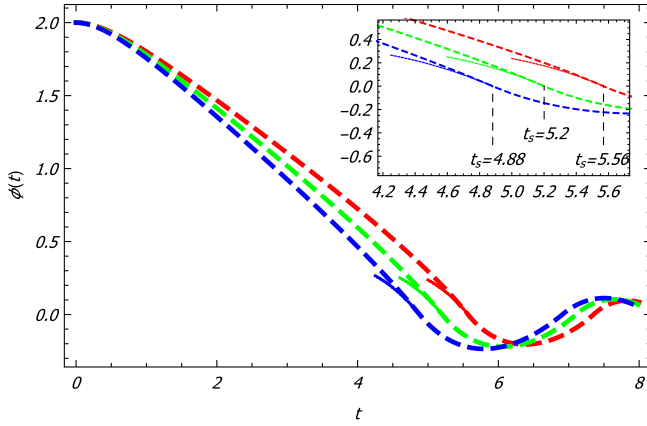


FIG. 11. Plot of numerical (dashed) and analytical (line) time evolution of the scalar field, for $n = 0.7$ (red), 0.8 (green), and 0.9 (blue). The two solutions for each n are consistent close to each singularity.

The quadratic term of $(t_s - t)$, in the expression of the scale factor (2.10), is now subdominant as the second derivative of the scale factor diverges. The only additional term of $(t_s - t)$ that can play an important role in the estimation of the Hubble parameter, is the linear term. Clearly, for the first derivative of (2.10), as $t \rightarrow t_s$ from below, the linear term dominates over all other terms, while the quadratic term is subdominant in the second derivative in the divergence of the q -term. Thus, in the case of the scalar-tensor quintessence models H remain finite and dominated by the term $b(t_s - t)$, while $\dot{H} \rightarrow \infty$ as $t \rightarrow t_s$.

C. Evolution with a perfect fluid

In the presence of a perfect fluid, the action is now the generalized action (2.1). The scale factor and the scalar field are of the form (2.28) and (2.11) respectively. The dynamical equations in the presence of a relativistic fluid become

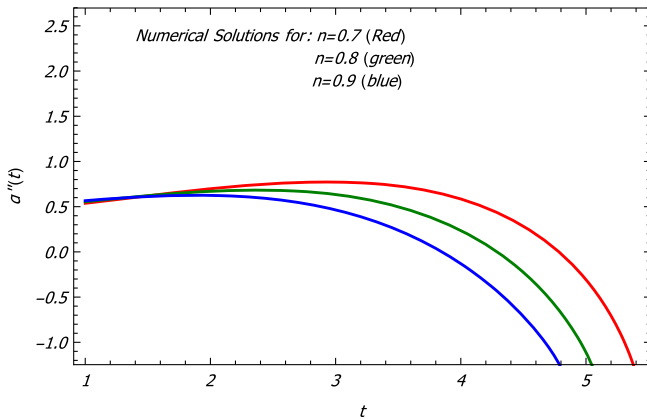


FIG. 12. Numerical solutions of the second time derivative of the scale factor for $n = 0.7, 0.8, 0.9$. Notice the divergence at the time of the singularity when the scalar field vanishes ($t_s = 5.56$ for $n = 0.7$, $t_s = 5.2$ for $n = 0.8$, $t_s = 4.88$ for $n = 0.9$).

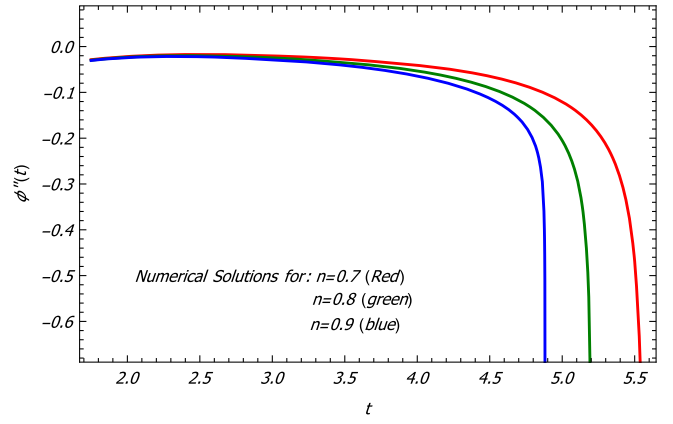


FIG. 13. Numerical solutions of the second time derivative of the scalar field for $n = 0.7, 0.8, 0.9$. Notice the divergence at the time of the singularity when the scalar field vanishes ($t_s = 5.56$ for $n = 0.7$, $t_s = 5.2$ for $n = 0.8$, $t_s = 4.88$ for $n = 0.9$).

$$3FH^2 = \frac{3\Omega_{0,m}}{a^3} + \frac{\dot{\phi}^2}{2} + V - 3H\dot{F} \quad (3.16)$$

$$\ddot{\phi} + 3H\dot{\phi} - 3F_\phi \left(\frac{\ddot{a}}{a} + H^2 \right) + V_\phi = 0 \quad (3.17)$$

$$-2F \left(\frac{\ddot{a}}{a} - H^2 \right) = \frac{3\Omega_{0,m}}{a^3} + \dot{\phi}^2 + \ddot{F} - H\dot{F} \quad (3.18)$$

The constraints for r, q as $t \rightarrow t_s$ from below, are the same as in the absence of the fluid i.e. $1 < r < 2$ and $1 < q < 2$, and following the steps of the Sec. III A we obtain

$$q = r, \quad (3.19)$$

$$r = n + 1, \quad (3.20)$$

and according to Eq. (3.19)

$$q = n + 1. \quad (3.21)$$

i.e. Eqs. (3.8), (3.10) and (3.11) respectively. Finally, the form of the evaluated expansion coefficients c, d, f, h is shown in the Appendix, and has been verified by numerical solution of the dynamical equations (see Appendix). As expected, for $\rho_{0m} = 0$, all coefficients reduce to the ones of the no fluid case.

TABLE III. Numerical and analytical values of the power-laws r, q . Clearly, there is consistency between numerical results and analytical expectations.

n	Numerical		Analytical	
	r	q	$r = n + 1$	$q = n + 1$
0.5	1.5 ± 0.0003	1.49 ± 0.0002	1.5	1.5
0.8	1.8 ± 0.03	1.8 ± 0.006	1.8	1.8

IV. CONCLUSION-DISCUSSION

We have derived analytically and numerically the cosmological solution close to a future-time singularity for both quintessence and scalar-tensor quintessence models. For quintessence, we have shown that there is a divergence of \ddot{a} and a GSFS singularity occurs (a_s, ρ_s, p_s remain finite but $\dot{p} \rightarrow \infty$), while in the case of scalar-tensor quintessence models there is a divergence of \ddot{a} and an SFS singularity occurs (a_s, ρ_s remain finite but $p_s \rightarrow \infty, \dot{p} \rightarrow \infty$). Importing a perfect fluid in the dynamical equations, in both cases, we have shown that this result is still valid in our cosmological solution.

These are the simplest nonexotic physical models where GSFS and SFS singularities naturally arise. In the case of scalar-tensor quintessence models, there is a divergence of the scalar curvature $R = 6(\frac{\ddot{a}}{a} + \frac{\dot{a}^2}{a^2}) \rightarrow \infty$ because of the divergence of the second derivative of the scale factor. Thus, a stronger singularity occurs in this class of models. Such divergence of the scalar curvature is not present in the simple quintessence case.

We have also shown the important role of the additional linear and quadratic terms of $t_s - t$ in the form of the scale factor as $t \rightarrow t_s$. However, in the scalar-tensor case the quadratic term becomes subdominant close to the singularity.

We have derived explicitly the relations between the coefficients of the linear, quadratic and diverging terms of the scale factor and the scalar field. We have shown that all coefficients of the fluid case (quintessence and scalar-tensor quintessence), reduce to those of the no fluid case for $\rho_{0m} = 0$, and all coefficients (except coefficient d) of the scalar-tensor models reduce to those of the simple quintessence, in the special case $\lambda = 0$ i.e. $F = 1$. Moreover, for quintessence models, we derived relations of the Hubble parameter, $\dot{H} = -3H^2$ (for the no fluid case) and $\dot{H} = \frac{3}{2}\Omega_{0,m}(1+z_s)^3 - 3H^2$ (for the fluid case), close to the singularity. These relations may be used as observational signatures of such singularities in this class of models.

Interesting extensions of the present analysis include the study of the strength of these singularities in other modified gravity models e.g. string-inspired gravity, Gauss-Bonnet gravity etc. [8,42] and the search for signatures of such singularities in cosmological luminosity distance and angular diameter distance data.

Numerical Analysis: The MATHEMATICA file that led to the production of the figures may be downloaded from here Ref. [91].

APPENDIX: PROOFS OF EQUATIONS

1. Relations among the expansion coefficients

a. Quintessence without matter

Substituting the expressions (2.10), (2.11), (1.9) for $a(t), \phi(t)$ and $V(\phi)$ in the dynamical Eqs. (2.4) and

(2.6), it is straightforward to obtain relations among the expansion coefficients as

$$f = \frac{b}{a_s} \sqrt{6} \quad (\text{A1})$$

$$c = -\frac{b^2}{a_s}. \quad (\text{A2})$$

$$h = -\frac{A f^{n-1}}{n+1} \quad (\text{A3})$$

$$d = \frac{A b \sqrt{6} f^{n-1}}{(n+1)(n+2)}. \quad (\text{A4})$$

Also Eq. (2.12) may be written explicitly as

$$hr(r-1)(t_s - t)^{r-2} = -A n f^{n-1} (t_s - t)^{n-1}$$

Thus, the constants $\mathcal{A}_1, \mathcal{A}_2$ are

$$\mathcal{A}_1 = hr(r-1) \quad (\text{A5})$$

$$\mathcal{A}_2 = -A n f^{n-1} \quad (\text{A6})$$

Similarly Eq. (2.14) may be written explicitly as

$$\frac{dq(q-1)(q-2)}{a_s} (t_s - t)^{q-3} = -fhr(r-1)(t_s - t)^{r-2}.$$

Thus, the constants $\mathcal{A}'_1, \mathcal{A}'_2$ are of the form

$$\mathcal{A}'_1 = \frac{dq(q-1)(q-2)}{a_s} \quad (\text{A7})$$

$$\mathcal{A}'_2 = -fhr(r-1). \quad (\text{A8})$$

b. Quintessence with matter

As in the previous case from the dynamical equations Eq. (2.25), (2.27) we find the corresponding expansion coefficients

$$f = \left[6 \frac{((a_s - 1)m - b)^2}{a_s^2} - 2 \frac{\rho_{0,m}}{a_s^3} \right]^{1/2}, \quad (\text{A9})$$

$$c = \frac{\rho_{0,m}}{4a_s^2} - \frac{1}{2}(a_s - 1)m(m-1) - \frac{[(a_s - 1)m - b]^2}{a_s}, \quad (\text{A10})$$

$$h = -\frac{A f^{n-1}}{n+1} \quad (\text{A11})$$

$$d = \frac{A f^{n-1}}{(n+1)(n+2)} \sqrt{6[(a_s-1)m-b]^2 - 2\frac{\rho_{0,m}}{a_s}}. \quad (\text{A12})$$

For $m = \rho_{0,m} = 0$ all coefficients reduce to the previous ones of the no fluid case as expected.

c. Scalar-tensor quintessence without matter

In this case the dynamical equations lead to the following relations among the expansion coefficients

$$f = -\frac{3\lambda b}{a_s} \pm \frac{\sqrt{3}\sqrt{b^2(2+3\lambda^2)}}{a_s} \quad (\text{A13})$$

$$d = \frac{1}{2}\lambda a_s h \quad (\text{A14})$$

$$c = -\frac{b^2}{a_s} + \frac{5}{4}\lambda b f. \quad (\text{A15})$$

$$h = -\frac{A f^{n-1}}{(n+1)(1+\frac{3}{2}\lambda^2)}. \quad (\text{A16})$$

We notice that all coefficients except d , reduce to those of Sec. II A for $\lambda = 0$. The reason that the coefficient d differs in scalar-quintessence is because in this case the divergence occurs in the second, instead of the third derivative of the scale factor.

Equation (3.7) is written explicitly, keeping only the dominant terms

$$2\frac{dq(q-1)}{a_s}(t_s-t)^{q-2} = \lambda h r(r-1)(t_s-t)^{r-2}.$$

Thus, the constants $\mathcal{B}_1, \mathcal{B}_2$ are

$$\mathcal{B}_1 = 2\frac{dq(q-1)}{a_s} \quad (\text{A17})$$

$$\mathcal{B}_2 = \lambda h r(r-1). \quad (\text{A18})$$

Similarly, Eq. (3.9) is written explicitly, keeping only the dominant terms

$$\left(\frac{3}{2}\lambda^2 + 1\right)r(r-1)(t_s-t)^{r-2} = -A n f^{n-1}(t_s-t)^{n-1}.$$

Thus, the constants $\mathcal{B}'_1, \mathcal{B}'_2$ are

$$\mathcal{B}'_1 = \left(\frac{3}{2}\lambda^2 + 1\right)r(r-1) \quad (\text{A19})$$

$$\mathcal{B}'_2 = -A n f^{n-1}. \quad (\text{A20})$$

d. Scalar-tensor quintessence with matter

As in the previous cases we use the relevant dynamical equation which in this case is Eq. (3.16) to obtain the relations among the expansion coefficients as

$$f = 3\lambda \left(m - \frac{b+m}{a_s} \right) \pm \sqrt{\frac{3a_s(2+3\lambda^2)(b+m-ma_s)^2 - 2\rho_{0,m}}{a_s^3}} \quad (\text{A21})$$

$$d = \frac{1}{2}\lambda a_s h, \quad (\text{A22})$$

$$c = \frac{\rho_{0,m}}{4a_s^2} - \frac{1}{2}(a_s-1)m(m-1) - \frac{[(a_s-1)m-b]^2}{a_s} - \frac{5}{4}\lambda f[(a_s-1)m-b], \quad (\text{A23})$$

$$h = -\frac{A f^{n-1}}{(n+1)(1+\frac{3}{2}\lambda^2)}. \quad (\text{A24})$$

Notice that for $\rho_{0,m} = 0$, all coefficients reduce to the ones in the absence of the fluid. Comparing them with the coefficients of quintessence models, we see that for $\lambda = 0$ they reduce to them except for the coefficient d . This occurs because d is the coefficient of the scale factor's diverging term. In quintessence models we have divergence of the third derivative of the scale factor, while in scalar-tensor models the second derivative of the scale factor diverges.

2. Proof of Eqs. (2.18) and (2.19)

The scale factor and its first and second derivative are

$$a(t) = a_s + b(t_s-t) + c(t_s-t)^2 + d(t_s-t)^q, \quad (\text{A25})$$

$$\dot{a} = -b - 2c(t_s-t) - dq(t_s-t)^{q-1}, \quad (\text{A26})$$

$$\ddot{a} = 2c + dq(q-1)(t_s-t)^{q-2}. \quad (\text{A27})$$

Close to the singularity Eqs. (2.10), (A26), and (A27) become

$$a(t) = a_s, \quad (\text{A28})$$

$$\dot{a} = -b, \quad (\text{A29})$$

and

$$\ddot{a} = 2c \quad (\text{A30})$$

respectively.

Substituting Eqs. (A28), (A29), and (A30) into the Hubble parameter and its derivative we have

$$H = -\frac{b}{a_s} \quad (\text{A31})$$

and

$$\dot{H} = \frac{2c}{a_s} - \frac{b^2}{a_s^2}. \quad (\text{A32})$$

Substituting Eqs. (A31) and (A32) in Eq. (A2) we obtain

$$\dot{H} = -3H^2. \quad (\text{A33})$$

In terms of the scale factor this equation becomes

$$aH_a + 3H(a) = 0,$$

where H_a denotes derivative of H with respect to a . The solution is

$$H(a) = a^{-3}$$

or, in terms of the redshift $H(z) = (1+z)^3$.

3. Proof of Eqs. (2.30) and (2.31)

$$H = \frac{(a_s - 1)m - b}{a_s} \quad (\text{A34})$$

and

$$\dot{H} = \frac{(a_s - 1)m(m - 1) + 2c}{a_s} - \frac{[(a_s - 1)m - b]^2}{a_s^2}. \quad (\text{A35})$$

Substituting Eqs. (A10) and (A34) in Eq. (A35) we find

$$\dot{H} = \frac{3\Omega_{0,m}}{2a_s^3} - 3H^2. \quad (\text{A36})$$

This may be written as

$$aH(a)H_a + 3H^2(a) - \frac{3\Omega_{0,m}}{2a^3} = 0$$

with solution

$$H^2(a) = \frac{\Omega_{0,m}}{a^3} \left[1 - \frac{1}{a^3} \right] + \frac{1}{a^6}.$$

In terms of the singularity redshift z_s this becomes

$$H^2(z_z) = \Omega_{0,m}(1+z_s)^3[1 - (1+z_s)^3] + (1+z_s)^6. \quad (\text{A37})$$

-
- [1] E. J. Copeland, M. Sami, and S. Tsujikawa, Dynamics of dark energy, *Int. J. Mod. Phys. D* **15**, 1753 (2006).
- [2] J. Frieman, M. Turner, and D. Huterer, Dark energy and the accelerating universe, *Annu. Rev. Astron. Astrophys.* **46**, 385 (2008).
- [3] A. G. Riess *et al.* (Supernova Search Team), Observational evidence from supernovae for an accelerating universe and a cosmological constant, *Astron. J.* **116**, 1009 (1998).
- [4] A. H. Jaffe *et al.* (Boomerang), Cosmology from MAXIMA-1, BOOMERANG and COBE / DMR CMB Observations, *Phys. Rev. Lett.* **86**, 3475 (2001).
- [5] S. W. Hawking and G. F. R. Ellis, *The Large Scale Structure of Space-Time*, Cambridge Monographs on Mathematical Physics (Cambridge University Press, Cambridge, 2011).
- [6] M. Davis, G. Efstathiou, C. S. Frenk, and S. D. M. White, The evolution of large scale structure in a universe dominated by cold dark matter, *Astrophys. J.* **292**, 371 (1985).
- [7] P. Bull *et al.*, Beyond Λ CDM: Problems, solutions, and the road ahead, *Phys. Dark Universe* **12**, 56 (2016).
- [8] S. Nojiri and S. D. Odintsov, Introduction to modified gravity and gravitational alternative for dark energy, *Theoretical physics: Current mathematical topics in gravitation and cosmology. Proceedings, 42nd Karpacz Winter School, Ladek, Poland, February 6-11, 2006*, eConf C0602061, 06 (2006); *Int. J. Geom. Methods Mod. Phys.* **04**, 115 (2007).
- [9] S. Nojiri and S. D. Odintsov, Modified gravity with negative and positive powers of the curvature: Unification of the inflation and of the cosmic acceleration, *Phys. Rev. D* **68**, 123512 (2003).
- [10] I. Zlatev, L.-M. Wang, and P. J. Steinhardt, Quintessence, cosmic coincidence, and the cosmological constant, *Phys. Rev. Lett.* **82**, 896 (1999).
- [11] S. M. Carroll, Quintessence and the rest of the world, *Phys. Rev. Lett.* **81**, 3067 (1998).
- [12] M. C. Bento, O. Bertolami, and A. A. Sen, Generalized chaplygin gas, accelerated expansion and dark energy matter unification, *Phys. Rev. D* **66**, 043507 (2002).
- [13] N. Bilic, G. B. Tupper, and R. D. Viollier, Unification of dark matter and dark energy: The Inhomogeneous chaplygin gas, *Phys. Lett. B* **535**, 17 (2002).
- [14] R. J. Scherrer, Phantom dark energy, cosmic doomsday, and the coincidence problem, *Phys. Rev. D* **71**, 063519 (2005).
- [15] S. Nesseris and L. Perivolaropoulos, The Fate of bound systems in phantom and quintessence cosmologies, *Phys. Rev. D* **70**, 123529 (2004).
- [16] L. Perivolaropoulos, Constraints on linear negative potentials in quintessence and phantom models from recent supernova data, *Phys. Rev. D* **71**, 063503 (2005).

- [17] A. Lykkas and L. Perivolaropoulos, Scalar-Tensor Quintessence with a linear potential: Avoiding the Big Crunch cosmic doomsday, *Phys. Rev. D* **93**, 043513 (2016).
- [18] *Mathematical Structures of the Universe*, edited by S. J. Szybka, M. Eckstein, and M. Heller (Copernicus Center Press, Kraków, 2014), pp. 99–117.
- [19] M. P. Dabrowski, Are singularities the limits of cosmology?, [arXiv:1407.4851](https://arxiv.org/abs/1407.4851).
- [20] I. Antoniadis, J. Rizos, and K. Tamvakis, Singularity—free cosmological solutions of the superstring effective action, *Nucl. Phys.* **B415**, 497 (1994).
- [21] G. N. Felder, A. V. Frolov, L. Kofman, and A. D. Linde, Cosmology with negative potentials, *Phys. Rev. D* **66**, 023507 (2002).
- [22] J. D. Barrow, Sudden future singularities, *Classical Quantum Gravity* **21**, L79 (2004).
- [23] L. Fernandez-Jambrina and R. Lazkoz, Geodesic behaviour of sudden future singularities, *Phys. Rev. D* **70**, 121503 (2004).
- [24] D. F. Mota and D. J. Shaw, Evading equivalence principle violations, cosmological and other experimental constraints in scalar field theories with a strong coupling to matter, *Phys. Rev. D* **75**, 063501 (2007).
- [25] V. K. Onemli and R. P. Woodard, Quantum effects can render $w < -1$ on cosmological scales, *Phys. Rev. D* **70**, 107301 (2004).
- [26] C. J. Fewster and G. J. Galloway, Singularity theorems from weakened energy conditions, *Classical Quantum Gravity* **28**, 125009 (2011).
- [27] Y.-I. Zhang and M. Sasaki, Screening of cosmological constant in non-local cosmology, *Int. J. Mod. Phys. D* **21**, 1250006 (2012).
- [28] K. Bamba, S. Nojiri, S. D. Odintsov, and M. Sasaki, Screening of cosmological constant for De Sitter Universe in non-local gravity, phantom-divide crossing and finite-time future singularities, *Gen. Relativ. Gravit.* **44**, 1321 (2012).
- [29] S. Nojiri, S. D. Odintsov, M. Sasaki, and Y.-I. Zhang, Screening of cosmological constant in non-local gravity, *Phys. Lett. B* **696**, 278 (2011).
- [30] K. Bamba, R. Myrzakulov, S. Nojiri, and S. D. Odintsov, Reconstruction of $f(T)$ gravity: Rip cosmology, finite-time future singularities and thermodynamics, *Phys. Rev. D* **85**, 104036 (2012).
- [31] J. D. Barrow, A. B. Batista, J. C. Fabris, M. J. S. Houndjo, and G. Dito, Sudden singularities survive massive quantum particle production, *Phys. Rev. D* **84**, 123518 (2011).
- [32] M. Bouhmadi-Lopez, Y. Tavakoli, and P. Vargas Moniz, Appeasing the Phantom Menace? *J. Cosmol. Astropart. Phys.* **04** (2010) 016.
- [33] M. Bouhmadi-López, C.-Y. Chen, and P. Chen, Eddington-Born-Infeld cosmology: A cosmographic approach, a tale of doomsdays and the fate of bound structures, *Eur. Phys. J. C* **75**, 90 (2015).
- [34] M. Bouhmadi-Lopez, C. Kiefer, B. Sandhofer, and P. Vargas Moniz, On the quantum fate of singularities in a dark-energy dominated universe, *Phys. Rev. D* **79**, 124035 (2009).
- [35] A. Kamenshchik and S. Manti, Classical and Quantum big Brake Cosmology for Scalar Field and Tachyonic Models, in *Proceedings, 13th Marcel Grossmann Meeting on Recent Developments in Theoretical and Experimental General Relativity, Astrophysics, and Relativistic Field Theories (MG13): Stockholm, Sweden, July 1-7, 2012* (World Scientific, Singapore, 2015) pp. 1646–1648.
- [36] A. Kamenshchik and S. Manti, Classical and quantum Big Brake cosmology for scalar field and tachyonic models, *Proceedings, Multiverse and Fundamental Cosmology (Multicosmofun'12): Szczecin, Poland, September 10-14, 2012*, *AIP Conf. Proc.* **1514**, 179 (2013).
- [37] A. Y. Kamenshchik and S. Manti, Classical and quantum Big Brake cosmology for scalar field and tachyonic models, *Phys. Rev. D* **85**, 123518 (2012).
- [38] M. P. Dabrowski, C. Kiefer, and B. Sandhofer, Quantum phantom cosmology, *Phys. Rev. D* **74**, 044022 (2006).
- [39] M. P. Dabrowski, K. Marosek, and A. Balcerzak, Standard and exotic singularities regularized by varying constants, *Proceedings, Varying fundamental constants and dynamical dark energy: Sesto Pusteria, Italy, July 8–13, 2013*, *Mem. Soc. Astron. Ital.* **85**, 44 (2014).
- [40] L. Fernandez-Jambrina and R. Lazkoz, Singular fate of the universe in modified theories of gravity, *Phys. Lett. B* **670**, 254 (2009).
- [41] A. Kamenshchik, C. Kiefer, and B. Sandhofer, Quantum cosmology with big-brake singularity, *Phys. Rev. D* **76**, 064032 (2007).
- [42] S. Nojiri and S. D. Odintsov, The Future evolution and finite-time singularities in F(R)-gravity unifying the inflation and cosmic acceleration, *Phys. Rev. D* **78**, 046006 (2008).
- [43] S. Nojiri and S. D. Odintsov, Is the future universe singular: Dark Matter versus modified gravity? *Phys. Lett. B* **686**, 44 (2010).
- [44] M. Sami, P. Singh, and S. Tsujikawa, Avoidance of future singularities in loop quantum cosmology, *Phys. Rev. D* **74**, 043514 (2006).
- [45] P. Singh and F. Vidotto, Exotic singularities and spatially curved Loop Quantum Cosmology, *Phys. Rev. D* **83**, 064027 (2011).
- [46] R. Penrose, Singularities and big-bang cosmology, *Q. J. R. Astron. Soc.* **29**, 61 (1988).
- [47] F. Briscese, E. Elizalde, S. Nojiri, and S. D. Odintsov, Phantom scalar dark energy as modified gravity: Understanding the origin of the Big Rip singularity, *Phys. Lett. B* **646**, 105 (2007).
- [48] L. P. Chimento and R. Lazkoz, On big rip singularities, *Mod. Phys. Lett. A* **19**, 2479 (2004).
- [49] P. H. Frampton, K. J. Ludwick, S. Nojiri, S. D. Odintsov, and R. J. Scherrer, Models for little rip dark energy, *Phys. Lett. B* **708**, 204 (2012).
- [50] P. H. Frampton, K. J. Ludwick, and R. J. Scherrer, Pseudo-rip: Cosmological models intermediate between the cosmological constant and the little rip, *Phys. Rev. D* **85**, 083001 (2012).
- [51] I. P. C. Heard and D. Wands, Cosmology with positive and negative exponential potentials, *Classical Quantum Gravity* **19**, 5435 (2002).
- [52] S. Elitzur, A. Giveon, D. Kutasov, and E. Rabinovici, From big bang to big crunch and beyond, *J. High Energy Phys.* **06** (2002) 017.

- [53] R. Giambò, J. Miritzis, and K. Tzanni, Negative potentials and collapsing universes II, *Classical Quantum Gravity* **32**, 165017 (2015).
- [54] V. Gorini, A. Yu. Kamenshchik, U. Moschella, and V. Pasquier, Tachyons, scalar fields and cosmology, *Phys. Rev. D* **69**, 123512 (2004).
- [55] T. Denkiewicz, Observational constraints on finite scale factor singularities, *J. Cosmol. Astropart. Phys.* **07** (2012) 036.
- [56] M. Bouhmadi-López, P. F. González-Díaz, and P. Martín-Moruno, Worse than a big rip?, *Phys. Lett. B* **659**, 1 (2008).
- [57] M. P. Dabrowski and T. Denkiewicz, Barotropic index w -singularities in cosmology, *Phys. Rev. D* **79**, 063521 (2009).
- [58] L. Fernandez-Jambrina, w -cosmological singularities, *Phys. Rev. D* **82**, 124004 (2010).
- [59] L. Fernandez-Jambrina and R. Lazkoz, Classification of cosmological milestones, *Phys. Rev. D* **74**, 064030 (2006).
- [60] F. J. Tipler, Singularities in conformally flat spacetimes, *Phys. Lett. A* **64**, 8 (1977).
- [61] A. Krolak, Towards the proof of the cosmic censorship hypothesis, *Classical Quantum Gravity* **3**, 267 (1986).
- [62] L. Perivolaropoulos, Fate of bound systems through sudden future singularities, *Phys. Rev. D* **94**, 124018 (2016).
- [63] W. Rudnicki, R. J. Budzynski, and W. Kondracki, Generalized strong curvature singularities and cosmic censorship, *Mod. Phys. Lett. A.* **17**, 387–397 (2002).
- [64] W. Rudnicki, R. J. Budzynski, and W. Kondracki, Generalized strong curvature singularities and weak cosmic censorship in cosmological space-times, *Mod. Phys. Lett. A* **21**, 1501–1510 (2006).
- [65] G. Hinshaw *et al.* (WMAP), Nine-Year Wilkinson Microwave Anisotropy Probe (WMAP) Observations: Cosmological Parameter Results, *Astrophys. J. Suppl.* **208**, 19 (2013).
- [66] S. Nojiri, S. D. Odintsov, and S. Tsujikawa, Properties of singularities in the (phantom) dark energy universe, *Phys. Rev. D* **71**, 063004 (2005).
- [67] J. D. Barrow, G. J. Galloway, and F. J. Tipler, The closed-universe recollapse conjecture, *Mon. Not. R. Astron. Soc.* **223**, 835 (1986).
- [68] J. D. Barrow, S. Cotsakis, and A. Tsokaros, A general sudden cosmological singularity, *Classical Quantum Gravity* **27**, 165017 (2010).
- [69] M. P. Dabrowski and K. Marosek, Regularizing cosmological singularities by varying physical constants, *J. Cosmol. Astropart. Phys.* **02** (2013) 012.
- [70] K. Marosek, M. P. Dabrowski, and A. Balcerzak, Cyclic multiverses, *Mon. Not. R. Astron. Soc.* **461**, 2777 (2016).
- [71] A. Kamenshchik, Z. Keresztes, and L. Á. Gergely, The paradox of soft singularity crossing avoided by distributional cosmological quantities, in *Proceedings, 13th Marcel Grossmann Meeting on Recent Developments in Theoretical and Experimental General Relativity, Astrophysics, and Relativistic Field Theories (MG13): Stockholm, Sweden, July 1-7, 2012* (World Scientific, Singapore, 2015), pp. 1847–1849.
- [72] Z. Keresztes, L. A. Gergely, and A. Yu. Kamenshchik, The paradox of soft singularity crossing and its resolution by distributional cosmological quantities, *Phys. Rev. D* **86**, 063522 (2012).
- [73] G. Kofinas, R. Maartens, and E. Papantonopoulos, Brane cosmology with curvature corrections, *J. High Energy Phys.* **03** (2003) 066.
- [74] G. Calcagni, Slow roll parameters in braneworld cosmologies, *Phys. Rev. D* **69**, 103508 (2004).
- [75] J. D. Barrow and A. A. H. Graham, Singular Inflation, *Phys. Rev. D* **91**, 083513 (2015).
- [76] J. D. Barrow and A. A. H. Graham, New singularities in unexpected places, *Int. J. Mod. Phys. D* **24**, 1544012 (2015).
- [77] L. Perivolaropoulos and C. Sourdis, Cosmological effects of radion oscillations, *Phys. Rev. D* **66**, 084018 (2002).
- [78] L. Perivolaropoulos, Equation of state of oscillating Brans-Dicke scalar and extra dimensions, *Phys. Rev. D* **67**, 123516 (2003).
- [79] M. C. Johnson and M. Kamionkowski, Dynamical and gravitational instability of oscillating-field dark energy and dark matter, *Phys. Rev. D* **78**, 063010 (2008).
- [80] N. A. Lima, P. T. P. Viana, and I. Tereno, Constraining recent oscillations in quintessence models with euclid, *Mon. Not. R. Astron. Soc.* **441**, 3231 (2014).
- [81] S. Dutta and R. J. Scherrer, Evolution of oscillating scalar fields as dark energy, *Phys. Rev. D* **78**, 083512 (2008).
- [82] J. D. Barrow, More general sudden singularities, *Classical Quantum Gravity* **21**, 5619 (2004).
- [83] J. D. Barrow and A. C. Ottewill, The stability of general relativistic cosmological theory, *J. Phys. A* **16**, 2757 (1983).
- [84] R. R. Caldwell and E. V. Linder, The Limits of quintessence, *Phys. Rev. Lett.* **95**, 141301 (2005).
- [85] R. J. Scherrer and A. A. Sen, Thawing quintessence with a nearly flat potential, *Phys. Rev. D* **77**, 083515 (2008).
- [86] S. Capozziello, S. Nesseris, and L. Perivolaropoulos, Reconstruction of the scalar-tensor lagrangian from a LCDM background and noether symmetry, *J. Cosmol. Astropart. Phys.* **12** (2007) 009.
- [87] M. P. Dabrowski, T. Denkiewicz, and M. A. Hendry, How far is it to a sudden future singularity of pressure? *Phys. Rev. D* **75**, 123524 (2007).
- [88] L. Perivolaropoulos, Crossing the phantom divide barrier with scalar tensor theories, *J. Cosmol. Astropart. Phys.* **10** (2005) 001.
- [89] S. Nesseris and L. Perivolaropoulos, The limits of extended quintessence, *Phys. Rev. D* **75**, 023517 (2007).
- [90] S. Nesseris and L. Perivolaropoulos, Crossing the phantom divide: Theoretical implications and observational status, *J. Cosmol. Astropart. Phys.* **01** (2007) 018.
- [91] <http://leandros.physics.uoi.gr/quint-singularities/math-quint.zip>.